



Age and stratigraphic context of *Pliopithecus* and associated fauna from Miocene sedimentary strata at Damiao, Inner Mongolia, China



Anu Kaakinen^{a,*}, Hayfaa Abdul Aziz^{a,b,1}, Benjamin H. Passey^c, Zhaoqun Zhang^d, Liping Liu^d, Johanna Salminen^{a,e}, Lihua Wang^{d,2}, Wout Krijgsman^b, Mikael Fortelius^a

^a Department of Geosciences and Geography, University of Helsinki, P.O. Box 64, Finland

^b Paleomagnetic Laboratory 'Fort Hoofddijk', Utrecht University, Budapestlaan 17, 3584 CD Utrecht, The Netherlands

^c Department of Earth and Planetary Sciences, Johns Hopkins University, Baltimore, MD 21218, USA

^d Key Laboratory of Vertebrate Paleontology and Human Origins of Chinese Academy of Sciences, Institute of Vertebrate Paleontology and Paleoanthropology, Chinese Academy of Sciences, 142 Xizhimenwai Street, 100044 Beijing, China

^e Department Physics, University of Helsinki, P.O. Box 64, Finland

ARTICLE INFO

Article history:

Received 7 July 2014

Received in revised form 18 November 2014

Accepted 21 December 2014

Available online 22 January 2015

Keywords:

Magnetostratigraphy

Fossil mammals

Pliopithecid primates

Palaeoenvironment

Neogene

Nei Mongol

ABSTRACT

Since the discovery of mammalian fossils in Central Inner Mongolia in the beginning of the 20th century, this area has produced a rich and diverse record of Miocene faunas. Nevertheless, the stratigraphy has remained poorly constrained owing to scattered faunal horizons and lack of continuous vertical exposures. Consequently, most age estimates of these Miocene sites are based on paleontological evidence alone, with very few sites having been dated independently.

Our field investigations in Damiao, in Siziwang Qi, Inner Mongolia have yielded more than 30 new fossiliferous localities from three horizons, including a pliopithecid fauna. This study presents the litho-, bio- and magnetostratigraphy of the Damiao area and provides age estimates for the three fossil-bearing horizons. The sedimentary sequence is interpreted as the remains of a fluvial system comprising channels, subaerially exposed floodplains and floodbasin environments. The two local stratigraphic sections measured and sampled for paleomagnetic analysis coincide with species-rich vertebrate fossil localities. The paleomagnetic results and faunal evidence suggest a correlation of lowermost fossil horizon (DM16) producing relatively rich small mammal assemblage to the early Miocene chron C6Ar or C6An.1r, roughly in 20–21 Ma age range. The pliopithecid locality level (DM01) represents latest middle Miocene and has an age estimate of about 12.1 Ma while the youngest localities (DM02) with cervoids and abundant and diverse small mammal fauna represents the earliest late Miocene with an age estimate of about 11.6 Ma.

Our magnetostratigraphic results confirm that the Damiao strata constitute one of the best sequences in Inner Mongolia with early, middle and late Miocene mammalian faunas in stratigraphic superposition. The results also provide constraints on the paleoenvironmental evolution and bioevents of the area. The occurrence of pliopithecid primates in the middle Miocene of Inner Mongolia suggests humid habitats and challenges the scenarios suggesting arid and highly seasonal conditions for Central Asia since Early Miocene. The presence of pliopithecids may also bear witness to locally humid environments and greater habitat heterogeneity than previously known in central Inner Mongolia.

© 2015 Elsevier Ltd. All rights reserved.

* Corresponding author. Tel.: +358 (0)294150819, +358 (0)504480215.

E-mail addresses: anu.kaakinen@helsinki.fi (A. Kaakinen), hayfaa@enresinternational.com (H. Abdul Aziz), bhpassey@jhu.edu (B.H. Passey), zhangzhaoqun@ivpp.ac.cn (Z. Zhang), liuliping@ivpp.ac.cn (L. Liu), johanna.m.salminen@helsinki.fi (J. Salminen), w.krijgsman@uu.nl (W. Krijgsman), mikael.fortelius@helsinki.fi (M. Fortelius).

¹ Present address: Enres International, Euclideslaan 201, 3584 BS Utrecht, The Netherlands.

² Present address: Yunnan Key Laboratory for Paleobiology, Yunnan University, 650091 Kunming, China.

1. Introduction

Our understanding of evolutionary processes and conditions of the past relies on successive fossil records and long sedimentary sequences. For Neogene fossil records, Central Inner Mongolia has been an area of great paleontological interest since the beginning of last century (e.g. Andersson, 1923; Teilhard de Chardin, 1926a,b; Andrews, 1932; see also Qiu Z.D. et al., 2013). Although housing numerous Neogene mammal sites, the localities are often

scattered and their stratigraphy is hampered by lack of continuous vertical exposures; the area is mostly rolling grassland and the degree of exposure is limited and fossil localities occur mainly as single faunal horizons.

Central Inner Mongolia was first explored in the 1920s by Swedish geologist J.G. Andersson, French palaeontologist P. Teilhard de Chardin, and the American Museum of Natural History Central Asian Expedition crews led by R.C. Andrews. These studies resulted in the discovery of two rich Neogene mammalian faunas, the middle Miocene Tunggur fauna (Andrews, 1932) and the late Miocene Ertemte fauna (Andersson, 1923). Since these pioneering studies, both faunal horizons have produced multiple large and small mammal localities (Qiu, 1996; Qiu and Storch, 2000; Wang et al., 2003; Qiu Z.D. et al., 2013), and a number of new localities producing rich faunas spanning most of the Neogene (Qiu et al., 2006; Wang et al., 2009). However, fossil records from the early Miocene (Xiejian and Shanwangian) of Inner Mongolia are relatively rare. One fauna is known from Sunitezuoqi (Meng et al., 1996), and a more recent was extracted from Aeorban strata (Wang et al., 2009), both are of the Shanwangian age.

The Damiao locality was discovered in 2006 by one of us (Z. Z.Q.), and during the following three years extensive field activities were undertaken. The focus was on paleontological studies, including screen washing and detailed excavations, and on stratigraphic studies in Neogene sediments. The field survey led to the recovery of more than 30 new fossiliferous localities, including a rich mammalian fauna with pliopithecoid material (Zhang and Harrison, 2008; Zhang et al., 2011a, 2011b; Wang and Zhang, 2011). The bulk of the vertebrate fossils and localities have been recovered from three main fossil horizons ranging from Xiejian to Early Bahean mammalian ages (Zhang et al., 2011a). Preliminary study on the successive faunas shows stable community structure and continuity of many lineages during the time interval investigated. In this paper we present the litho-, bio- and magnetostratigraphy of the Damiao area. The results provide chronologic control for the Damiao fossil occurrences as well as constraints on the paleoenvironmental evolution and bioevents of the area.

2. Geological setting

The sediments of the Damiao site crop out along the Sharamurun river valley near the Damiao village of Shiziwang Banner, north of the Daqing Shan and ca. 65 km northwest from the Wulanhua town (Fig. 1). The landscape in this area is characterized by undulating terrain with elevations ranging between 1250 and 1350 m a.s.l. Structurally the Damiao area lies near the southwestern margin of the Erlian Basin which is part of late Mesozoic extensional basin system in the China-Mongolian border region (Meng et al., 2003). These individual basins are internally composed of isolated sub-basins of different scales. They are characteristically shallow in nature and separated from one another by intrabasinal highs. The basin system is dominantly filled with late Mesozoic fluvio-lacustrine sequences (Lin et al., 2001; Meng et al., 2003) that produce diverse dinosaur fossils. The Erlian Basin also carries a well-developed succession of mainly siliciclastic Cenozoic deposits (Bureau of Geology and Mineral Resources of Nei Mongol Autonomous region, 1991), famed for its mammalian fauna. The strata are entirely terrestrial.

The Erlian basin is floored by volcanic rocks and late Mesozoic sediments containing abundant volcanic intercalation as a result of extensive volcanism during the late Jurassic to Early Cretaceous times (Meng et al., 2003). Basalt sheet-flows and cinder cones of tholeiitic affinities have been reported also from the Neogene sequences of central Inner Mongolia (Luo and Chen, 1990; Xu and Ma, 1992). However, so far only two fossiliferous localities,

Pliocene Gaotege and late Miocene Baogedawula can be associated with basalts (Qiu et al., 2006).

3. Sedimentology

3.1. Methods

Two representative sedimentary sequences were logged using a Jacob's staff and described in the field from freshly exposed surfaces by applying the conventional methods of lithofacies analysis. In case of important fossil find localities and in outcrops where significant lateral variation was observed, multiple sections were investigated. Examination of hand specimens and thin sections from selected samples provided additional data for facies analysis. Grain sizes for selected samples were determined in the laboratory using a Malvern Mastersizer 2000. Paleocurrent indicators and sedimentary structures were measured to constrain dispersal pattern and locate source areas. Colors were obtained by comparison to Munsell™ Color soil charts. The relative amount of CaCO₃ in the sediment was estimated in the field with diluted hydrochloric acid.

The elemental composition and structure of carbonate concretions was determined by microprobe analysis. The mineralogy was determined by X-ray diffraction (XRD) analysis for powdered bulk samples.

3.2. Stratigraphic sections: descriptions and interpretations

The outcrop area and fossil sites around Damiao can be divided into the western and eastern sides, separated by the Wulanhua-Damiao motorway (Fig. 1). The bulk of the vertebrate fossils, including all of the pliopithecoid primate remains, have been recovered here, except for a few fossil localities, which occur several kilometers north (DM07, 08, 17, 18, 28), east (DM05, 06) and south (DM26) from Damiao. The western part of the Damiao area (Fig. 1) includes, for instance, fossil localities DM10, 14, 15, 16, 22, 23, 30, 31; the eastern part comprises the localities DM01, 02, 03, 09, 11, 12 and 13. The deeply weathered granitic basement crops out on both sides and the overlying strata are generally flat-lying.

3.2.1. Western section

The logged western section is exposed along the eastern bank of an ephemeral tributary, is about 26–30 m thick overall, and can be conveniently divided into two lithologically distinct parts (Figs. 2a and 3). The lower portion of the section is 15.5 m thick and is characterized by the prevalence of red (2.5YR 4/6) mudstones, commonly with a blocky weathering appearance. Grain sizes are typically clay or fine silt, some horizons contain scattered sand grains. In all, sand-graded material is a relatively minor constituent, except thin sand beds that occur at several levels in the sequence. These sandstone beds are laterally discontinuous with sharp upper and lower bedding surfaces. Mudstones have mostly massive appearance on a weathered surface, although thin, mm-scale horizontal lamination is observed locally. Slickensides, manganese nodules and calcium carbonate accumulation as layers and as nodules are discernable throughout the sequence. Some fine-scale alternation of red and green coloration is discernable in the lower portion of this interval.

Fossil locality DM16 occurs within a 1 m thick horizontally laminated claystone horizon in the lower part of the sequence, where desiccation features are present as small sandstone-filled cracks. The fossils are well preserved but fragmented, comprising mainly small mammal skeletal elements and some isolated teeth, although large mammal remains and gastropods have also been discovered.

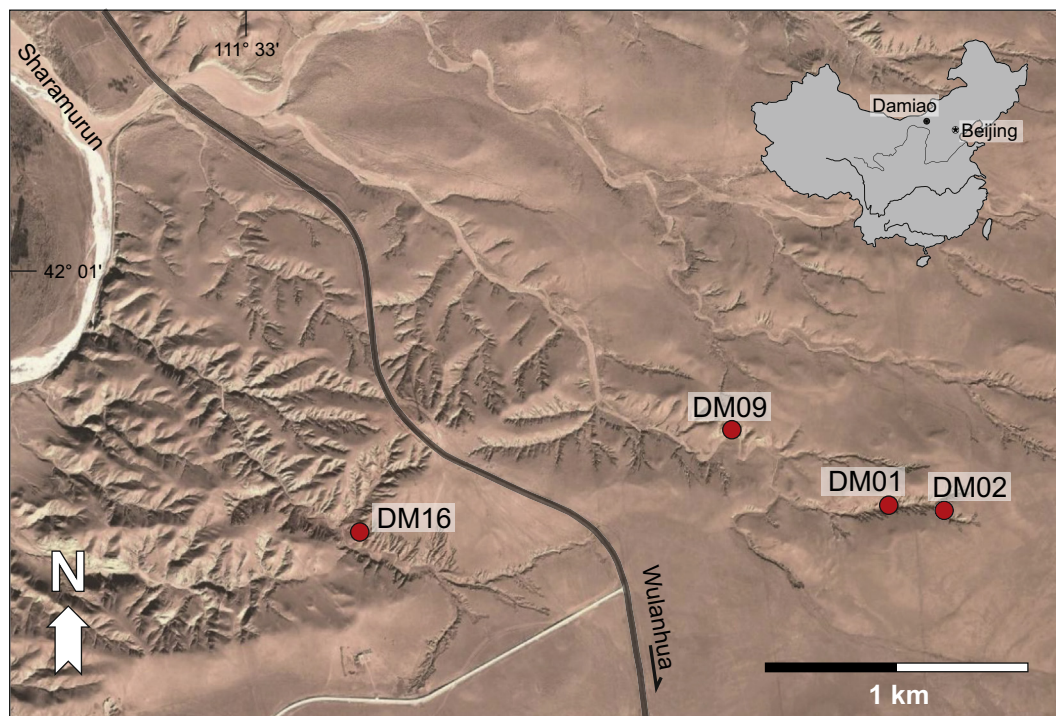


Fig. 1. Location map for the main Miocene fossil localities in Damiao area.

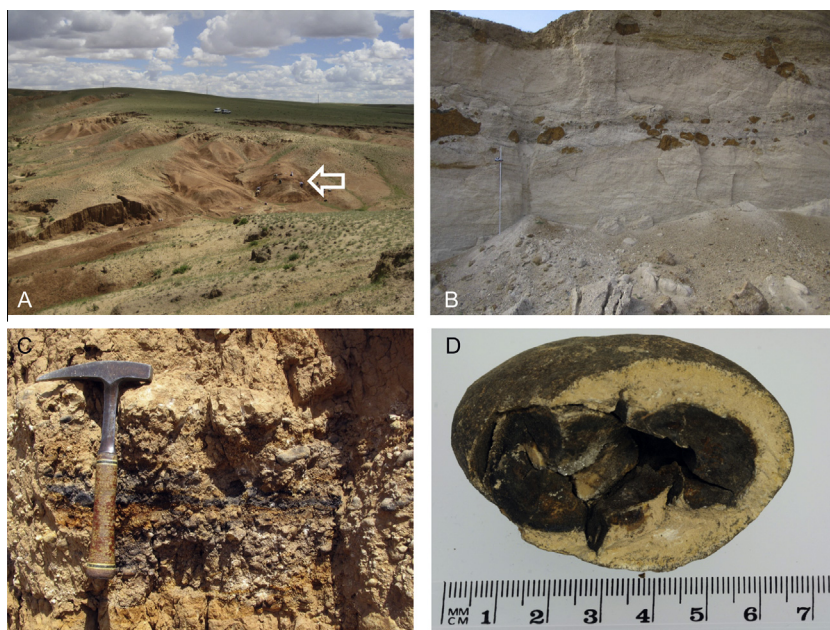


Fig. 2. (A) The western section, looking northeast. Arrow indicates locality DM16. (B) Overview of part of outcrop in the lowermost eastern section, showing trough cross bedded sand and gravel beds with rip-up clasts. The Jacob's staff on the left is 1.8 m high. (C) Detailed view of carbonate nodule conglomerate at locality DM01 level with black and rust staining. (D) Carbonate nodule clast in the conglomerate at DM01 level.

The upper part in the western section is demarcated by a lithologic transition at ca. 15.5 m where the red mudstones are erosionally truncated by a complex of sandstones and conglomerates. The lateral extent of this coarse-grained complex is at least 250 m, although individual beds are more restricted. The interbedded sheet-like bodies of fine-grained deposits also differ from the underlying red mudstones by their coarser grain sizes (typically coarse silt and sandy silt) and yellowish red (5YR 5/8) color. The

notable difference in sediment color is also evident on the opposite bank of the ephemeral river, where the red mudstones are directly overlain by yellowish siltstones.

The conglomerates in the upper part of the sequence are characteristically stratified and clast supported with a calcareous matrix. Although generally well-sorted there are horizons within the conglomerates that exhibit poor sorting. Clasts are mostly subangular. The conglomerates typically have an erosional,

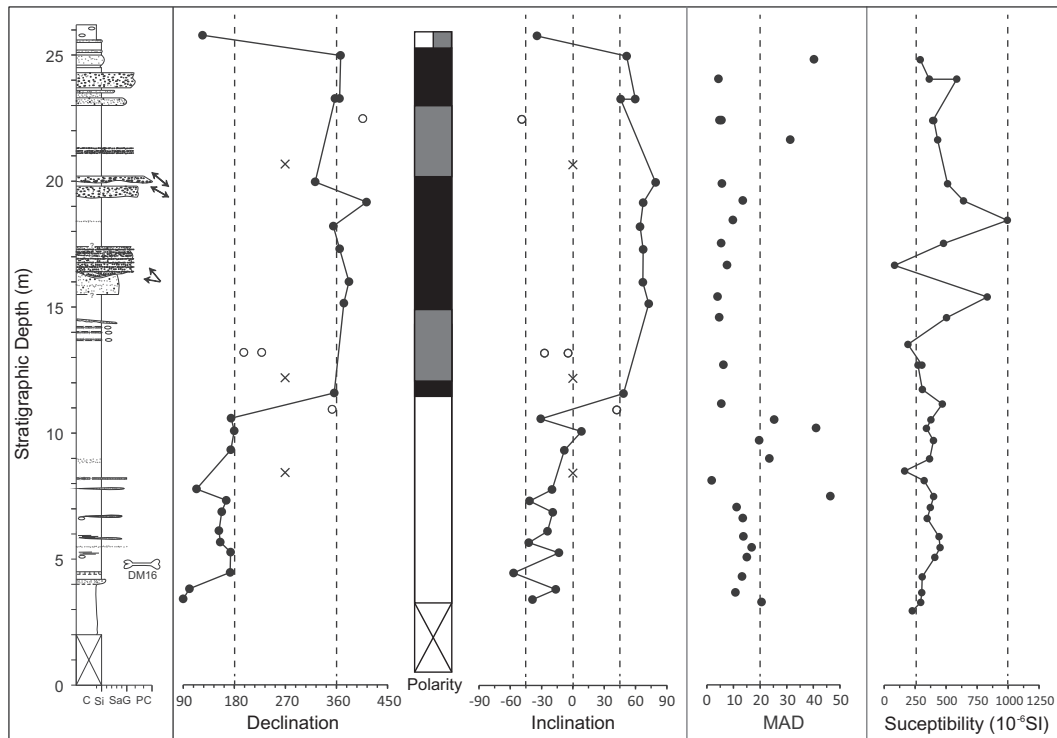


Fig. 3. Lithological column and palaeomagnetic analysis results of the Western (locality DM 16) section. The main fossil locality is indicated next to the lithological column. Black arrows denote paleocurrent directions (north oriented toward top of page). In the declination and inclination records, the black (white) dots represent reliable (unreliable) ChRM directions after thermal (and alternating field) demagnetization. The crosses represent non-interpretable directions. The polarity column shows the normal (black) and reversed (white) magnetozones. The gray shaded zones represent undefined polarity. The MAD shows the mean angular deviation with cut-off at 20°. The initial susceptibility for each sample is given.

undulating base and lack well-developed fining-upward trend. Some beds (e.g. the pebble conglomerate at 20 m level) have abundant intraformational siltstone clasts on lower boundaries.

The stacked sandstone and conglomerate bed at 15.5–17.5 m is made up of pebbly, coarse grained sandstone overlain by pebble-granule conglomerate interfingering with coarse and medium sandstones. Paleocurrents were measured from the associated planar cross beds, and the results indicate flow toward west – northwest.

Between ca 19.5 and 21.5 m in the measured sequence pebble granule conglomerates and thin pebble lags are present which correlate laterally with ca. 2–3 m thick trough and planar cross-stratified unit of very coarse sand and conglomerates. The cross-sectioned surface exhibits a convex upward upper bounding surface. Local paleocurrent evidence from trough trends show a generally WNW–ESE oriented flow.

Alternating centimeter- to decimetre-thick beds of mainly silt- and sandstones with subordinate clays and conglomerate beds characterizes the interval between 23 and 26 m. The beds are typically gritty; the contacts are distinctive but non-erosional. The silt and clay-dominated parts commonly contain small carbonate nodules few mm to cm size.

The sequence ends with poorly exposed conglomeratic bed, with thickness of at least 3 m.

3.2.2. Eastern section

The steep river bank around locality DM09 makes up the basal part of the eastern sequence and provides ca. 13 m of vertical section and laterally continuous exposure for about 200 m. The exposure continues southeast toward the locality DM01 gully, although the quality of outcrop exposure generally deteriorates in this direction. The sands higher up in the section, ca. 400 m SE from the DM09, are poorly exposed but are laterally equivalent to the basal

sand and conglomerate units of DM09 area. The upper portion of the eastern succession (ca. 13–42 m level) comprising the localities DM01, 02 and 13, are exposed above these sands in gently undulating slopes along the W–E trending small gully.

Gray, poorly cemented sandstones and conglomerates in the DM09 vicinity mostly overlie curved erosional surfaces and are mainly trough and planar cross-stratified in sets ranging from 10 cm to several decimetres in thickness (Figs. 2b and 4). Sets typically become finer and thinner toward the top of units. Most conglomerate clasts are subangular to sub-rounded, granule- to pebble-grade in size with some cobble-rich horizons and lags. The fabric is entirely clast-supported. The sands are medium to very coarse-grained and moderately sorted; the constituent grains are mainly quartz and potassium feldspars.

The lowermost part, ca. 6 m thick, contains abundant siltstone clasts and blocks varying from mm size to several decimetres in size, in addition to a few outsized blocks exceeding 1 m. These siltstone clasts are angular in shape, and typically concentrated in basal parts of individual beds but are also irregularly dispersed throughout.

Paleocurrent measurement from this lower portion of the succession are generally based on foreset dip directions and trough trends. Although there is some spread in the paleocurrent orientation, in general they indicate a northerly to northeasterly flow. Fossil vertebrate remains (locality DM09), including specimens of *Stephanoceras* sp. occur in the lower few meters of the section.

From ca. 13 to 23.5 m the succession comprises predominately beds of fine to coarse grained sandstones up to 1 m thick, interbedded with siltstones. Pebble beds and horizons are locally present. Within this interval, finer-grained sediments become increasingly dominant up-section. The coarser sandstones are massive or exhibit trough and planar cross-stratification, with planar cross-stratification at ca. 15-m-level giving paleocurrent directions to

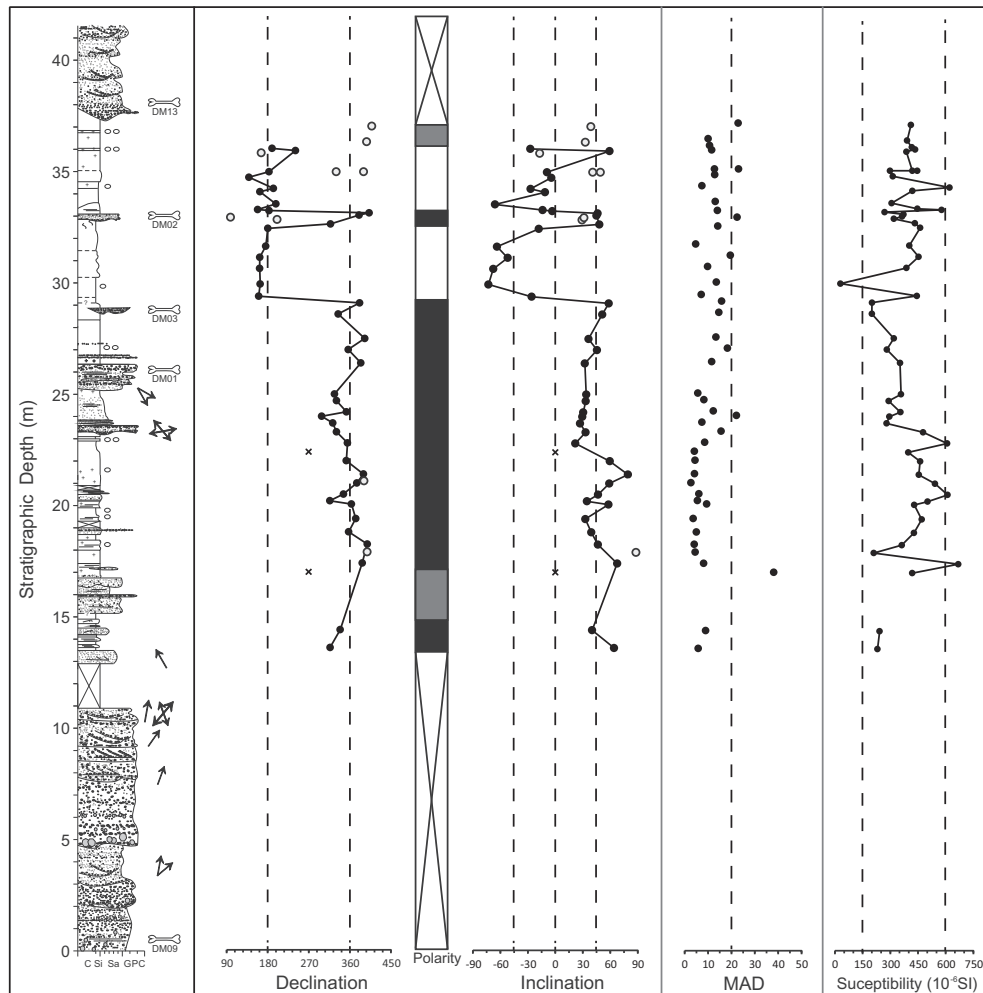


Fig. 4. Lithological column and palaeomagnetic analysis results of the Eastern (localities DM01 02) section. See caption to Fig. 3.

NW. The siltstone beds are commonly calcareous, internal structures include horizontal lamination and ripple-cross lamination. Nodular calcrete beds are developed at siltstones in the upper portion of the succession. Most contacts within this package are sharp, although some thicker sand beds have erosive bases with rip-up clasts.

The next interval extends from ca. 23.5 m to ca 29 m and comprises two clast-supported conglomerate units (at ca 23.5 and 26 m level) that are lithologically distinctive from the underlying coarse-grained deposits by having well-rounded clasts almost exclusively consisting of pedogenic carbonate nodules (Fig. 2c and d). The pedogenic nature of the clasts in these beds has been proven by the occurrence of rhizocretions in thin section. Carbonate nodules range generally from 1 to 6 cm, although coalesced forms up to 10 cm in diameter are found. Microscopically, carbonate nodules are micritic with occasional fractures and voids that were later filled by sparite crystals.

These conglomerate beds are tabular in the outcrops, with low-relief erosional bases and no significant change laterally over a distance of 60 m. The lowermost nodule conglomerate is up to 60 cm in thickness while the upper averages 1–1.5 m. Both are characterized by bedded heterolithic granule and pebble-grade nodule beds with minor amounts of medium to coarse-grained sandstone interbeds and lenses where trough and planar cross-beds are discerned. Matrix is generally poorly sorted silty sand which is often calcareous in the lower conglomerate. Overall the conglomerate outcrops

show black and rust color which comes from manganese and iron (goethite) staining on the nodules and matrix. The black staining is especially prominent in the upper unit, where the carbonate nodules have exclusively black coating and the matrix is very smeary.

Paleocurrent data were collected using asymmetrical ripple lamination and trough trends. Troughs trend W–E and NW–SE, whereas lee slopes of current ripples give paleocurrents toward the ESE–SSE.

The richest vertebrate locality (DM01) also occurs in the conglomerate bed at ca 26 m level, with over thousand bones and teeth concentrated at different levels of this unit. In addition to pliopithecoid molars, the vertebrate remains include both large and small mammals. Most elements are dissociated. The preservation status is, as a whole, characterized by well-preserved small mammal remains and pliopithecoid molars, while large mammal remains show more abrasion and breakage.

The fine-grained deposits associated with the nodule conglomerate units are mainly composed of well-sorted fine sands and silts exhibiting thin parallel lamination and cross-lamination. Lamination is less preserved in the siltstones overlying the DM01 where relict thin lamination is observed only locally. The color of these deposits varies between reddish yellow (7.5YR 6/6) to light brown (7.5YR 6/4). The siltstones overlying DM01 are calcareous throughout the entire profile; pedogenic carbonate concretions are present as separated ribbons of reworked nodules with manganese coating as well as in situ carbonate nodules concentrated as horizons.

At the top of this interval (at ca. 29 m level), a conglomerate overlies siltstones with an erosional basal contact. Due to the very poor exposure, it has an unknown lateral extent, thickness is approximately 0.5 m. Contrary to the underlying conglomerates, this unit comprises mainly quartz clasts with subordinate carbonates. Most clasts are granule or small pebbles in size, angular to subrounded, in a matrix of calcareous siltstone. A low density bone occurrence (DM03) is found in this conglomerate.

The interval between the localities DM03 and DM02 (ca. 29–33 m) includes beds of structureless red brown clay- and siltstone. Apart from few indurated nodules, the siltstone matrix is leached of carbonates. Slickensides are associated with the clayey bed in the topmost part of the succession.

The fossil locality DM02 occurs in an approximately 20 cm thick sandstone that rests upon the mudstones with an erosional lower contact. The sandstone is poorly sorted with angular clasts varying from very fine sand to granules in size. Faint bedding was observed within the small exposed area of few meters of lateral extent. This unit has yielded rich collection of small mammals consisting almost exclusively of teeth. Overlying the DM02 is a 4–5 m thick mudstone sequence showing subtle changes in color, texture and degree of CaCO₃ content.

Coarse grained sands and granules at 38–42 m level form laterally continuous unit that caps the whole succession. The dominant sedimentary structure is trough cross-stratification. The base of the unit displays curved erosional relief with rip up clasts concentrated at the base. Two fossil localities, DM12 and DM13, were found from these widely distributed sands. The fossiliferous level has yielded ostrich shells, long bones such as ribs, and a rhino tooth. The bones show typically black staining.

3.3. Depositional environments

On the basis of sedimentological evidence presented above, we interpret the Damiao sequence as the remains of a fluvial system comprising channels, sub-aerially exposed floodplains and, to a lesser extent, ephemeral/marginal lacustrine environments.

The most prominent coarse-grained deposits occur in the lower part of the eastern section. The thick sequence of sandstones and conglomerates in with pervasive cross-stratification and lack of paleosol development indicate continual influence of flowing water and mark the presence of a major paleo-river in the area. The paleocurrent measurements reflect a general trend of the fluvial drainage system toward the north – northeast, equal to the modern topography and flow directions. The absence of lateral accretion features and relatively unidirectional flow indicate a low-sinuosity fluvial system.

Minor conglomerates and coarse sandstone beds (characteristically less than 2 m thick) commonly punctuate the fine-grained overbank deposits in both western and eastern sections. These minor-coarse grained sediments typically with large width/thickness ratios are interpreted as small channels and sheet flow deposits resulting from episodic flood discharges. The nodule conglomerates at ca. 25 m level also results from the avulsive emplacement of channels reworking and concentrating the underlying calcic paleosols. Sedimentological features supporting the interpretation that the nodule conglomerate represents a re-worked calcic palaeosol include interbeds of trough-cross bedded sandstone and the scoured basal surface that truncates a pre-existing floodplain deposits (Van Itterbeek et al., 2007).

The fine-grained overbank deposits in Damiao comprise two types (1) lithologically heterogeneous, bedded fine-grained silts and sands, (2) a variety of mainly structureless claystones and clayey siltstones that generally display evidence of more intense pedogenic development. The lithologically heterogeneous intervals are typical for proximal floodplain areas with frequent sheet splays

and more rapid aggradation (e.g. Kraus and Gwinn, 1997) whereas the massive clayey silt-dominated portion of this spectrum represents more distal floodplain deposits. Red coloration in these fines indicates oxidizing conditions and low water tables. The fine grained member comprising the lower part of the western section marks the most distal facies of the fluvial system and is attributed to flood basin environments. The fine grain sizes, absence of evidence for tractional flow and, in places, the fissile texture indicate settling of suspended sediment from slow moving or stagnant water (e.g. Miall, 1996; Eberth and Miall, 1991). The horizontally laminated mudstones at fossil locality level DM16 with desiccation cracks and features indicative of incipient paleosol development (e.g. slickensides, carbonate precipitates, mottling, root traces) indicate sub-aerial exposure and suggest that these deposits may represent ephemeral water bodies. The lack of evaporites and presence of gastropods, frog, and snake remains in the fossil fauna suggests a fresh water setting.

4. Mammalian biostratigraphy

The fossil material was collected on surface outcrops, prospecting and by dry screening (localities DM01 and DM02); systematic sampling was carried out at DM16. In total, more than 20 fossil localities were found. Most of the fauna comes from a set of localities from three stratigraphic levels. The specimens are stored in the Institute of Vertebrate Paleontology and Paleoanthropology, Beijing.

DM16 level (also DM10, DM14, DM15, DM22, DM23, DM30, DM31, which are found in the same level within few meters of DM16). 21 species of 13 families in 6 orders are tentatively identified (Table 1). Perissodactyls are poorly represented by tooth fragments and broken bones, making further identification difficult. Artiodactyls are relatively better preserved with teeth, postcranials and some antler fragments recovered. Four species can be identified: *Lagomeryx* sp. indet., *Stephanocemas* sp. nov., *Micromeryx* sp. indet. and a large unidentified species of Cervidae. A partial broken mandible of Mustelidae gen. et sp. indet. is the only record of carnivores. Contrary to the rarity of large mammals, small mammal remains are relatively abundant at this horizon. The assemblage is dominated by *Metaxallarix gaolanshanensis*, *Sinolagomys ulunguensis*, *Tachyoryctoides* sp. nov., *Prodistylomys wangae*, *Distylomys* cf. *D. tedfordi*, *Sinodonomys* sp. indet., *Plesiosminthus* sp. indet., *Heterosminthus* sp. indet., *Pseudotheriodomys* sp. nov., and Eomyidae gen. et sp. nov. This fauna is characterized by the dominance of genera commonly found from the Oligocene, such as *Tachyoryctoides*, *Prodistylomys*, *Distylomys*, *Plesiosminthus*, *Pseudotheriodomys*, *Sinolagomys*, *Metaxallarix*, *Amphelchinus*, although represented by more derived species. *Sinolagomys ulunguensis* is the latest record of the genus, otherwise only recorded from early Miocene (Tong, 1989; Qiu et al., 2006; Wang et al., 2009). *Metaxallarix gaolanshanensis* is also a derived species only previously found from lower Miocene strata (Qiu and Gu, 1988). *Tachyoryctoides* sp. nov. is much smaller than the other Oligocene species and likely to represent the latest record of the genus. *Sinodonomys* was recently discovered from the Lower Auerbar fauna of early Miocene age (Kimura, 2010). By the taxonomic composition, this fauna is similar to the Lower Auerbar fauna (Wang et al., 2009), with most of the taxa shared, although with the notable exception of *Democricetodon*. A similar fauna was also recovered from Suosuoquan Zone III, Xinjiang Junggar basin (Meng et al., 2006). Both faunas are characterized by abundance of *Sinolagomys unluunguensis* (Meng et al., 2006). *Metaxallarix junggarensis* shows a similar evolutionary level with *M. gaolanshanensis* (Bi, 1999). Compared with the Xiejia fauna, considered earliest Miocene in age (Li and Qiu, 1980), the DM 16 fauna has a diversified cervoid assemblage. On the other hand,

Table 1

Mammalian taxa recorded from the three main localities in Damiao.

Locality	Age	Large mammals	Small mammals
DM16	20–21 Ma	Carnivora Mustelidae gen. et sp. indet. Artiodactyla Cervidae <i>Lagomeryx</i> sp. indet. <i>Stephanocemas</i> sp. nov. Cervidae gen. et sp. indet. Moschidae <i>Micromeryx</i> sp. indet. Perissodactyla Rhinocerotidae gen. et sp. indet.	Lagomorpha Ochotonidae <i>Sinolagomys ulunguensis</i> Rodentia Sciuridae <i>Kherem</i> cf. <i>K. asiatica</i> Dipodidae <i>Sinodonomys</i> sp. indet. <i>Plesiosminthus</i> sp. indet. <i>Heterosminthus</i> sp. indet. Muridae <i>Tachyoryctoides</i> sp. nov. Eomyidae <i>Pseudootheridomys</i> sp. nov. Eomyidae gen. et sp. nov. Ctenodactylidae <i>Prodistylomys wangae</i> <i>Distylomys</i> cf. <i>D. tedfordi</i> Lipotyphla Erinaceidae <i>Metexallerix gaolanshanensis</i>
DM01	12.1 Ma	Carnivora Mustelidae gen. et sp. indet. Felidae gen. et sp. indet. Primates Pliopithecidae gen. et sp. indet. Artiodactyla Cervidae <i>Stephanocemas</i> sp. I–III <i>Euprox altus</i> Moschidae <i>Micromeryx</i> sp. indet. Perissodactyla Rhinocerotidae gen. et sp. indet. Anchitheriinae gen. et sp. indet. Proboscidea Proboscidea gen. et sp. indet.	Lagomorpha Ochotonidae <i>Desmatolagus moergenensis</i> <i>Bellatona</i> cf. <i>B. forsythmajori</i> <i>Bellatonoides eroli</i> <i>Ochotona</i> cf. <i>O. lagreli</i> Rodentia Aplodontidae <i>Ansomys</i> sp. indet. Aplodontidae gen. et sp. indet. Sciuridae <i>Atlantoxerus orientalis</i> <i>Eutamias</i> sp. indet. Castoridae <i>Steneofiber hesperus</i> Dipodidae <i>Heterosminthus orientalis</i> <i>Protalactaga grabaui</i> Muridae <i>Gobicricetodon flynni</i> Gobicricetodontinae gen. et sp. nov. <i>Plesiodipus</i> sp. indet. <i>Democricetodon</i> sp. indet. <i>Prosiphneus</i> sp. indet. Myoxidae <i>Microdyromys</i> sp. indet. Eomyidae <i>Leptodontomys</i> sp. indet. <i>Keramidomys</i> sp. indet. Lipotyphla Erinaceidae <i>Mioechinus?</i> <i>gobiensis</i> Talpidae <i>Desmanella storchii</i>
DM02	11.6 Ma	Artiodactyla Cervidae <i>Stephanocemas</i> sp. indet. <i>Euprox altus</i> Moschidae <i>Micromeryx</i> sp. indet.	Lagomorpha Ochotonidae <i>Desmatolagus</i> sp. indet. <i>Bellatona forsythmajori</i> <i>Ochotona</i> sp. indet. <i>Alloptox</i> sp. indet. Rodentia Aplodontidae Aplodontidae gen. et sp. indet. Castoridae Castoridae gen. et sp. indet. Dipodidae <i>Lophocricetus</i> sp. indet. <i>Eozapus</i> sp. indet. <i>Protolactaga</i> sp. indet. Gliridae Gliridae gen. et sp. indet. Cricetidae

Table 1 (continued)

Locality	Age	Large mammals	Small mammals
			Cricetidae gen. et sp. nov.
			Muridae
			<i>Gobicricetodon</i> sp. indet.
			<i>Prosiphneus qiui</i>
			<i>Nannocricetus wuae</i>
			Eomyidae
			Eomyidae gen. et sp. indet.
			Lipotyphla
			Erinaceidae
			<i>Mioechinus</i> sp. indet.
			Talpidae
			Talpidae gen. et sp. indet.

small size and primitive characters of these cervoids suggest that they are of earlier age than those of the Shanwangian faunas.

DM01 level (also DM03): There are more than 30 species found from locality DM01 (Table 1), including one species of pliopithecids, two species of insectivores *Mioechinus? gobiensis*, and *Desmanella storchi*, four species of lagomorphs: *Desmatolagus moergenensis*, *Bellatona* cf. *B. forsythmajori*, *Bellatonoides eroli*, *Ochotona* cf. *O. lagreli* and more than 15 species of rodents: *Atlantoxerus orientalis*, *Eutamias* sp. indet., *Heterosminthus orientalis*, *Protolactaga grabau*, *Gobicricetodon flynni*, *Gobicricetodontinae* gen. et sp. nov., *Plesiodipus* sp. indet., *Prosiphneus* sp. indet., *Democricetodon* sp. indet., *Ansomys* sp. indet., *Aplodontidae* gen. et sp. indet., *Stenofiber hesperus*, *Leptodontomys* sp. indet., *Keramidomys* sp. indet., and *Microdyromys* sp. indet. Artiodactyls are represented by 5 taxa of cervoids: one species of *Micromeryx*, *Euprox altus* and three forms of *Stephanocemas*. One small-sized mustelid carnivore is also present. Perissodactyls and proboscideans are rare and represented by very fragmentary material. In contrast to the DM16 fauna, this fauna is composed of taxa from extant families without Paleogene members. Except *Desmatolagus morgenensis*, a possible survivor of an Oligocene lineage, all genus-level taxa are of Miocene age. At the species level, *Mioechinus? gobiensis*, *Desmanella storchi*, *Bellatona forsythmajori*, *Desmatolagus morgenensis*, *Atlantoxerus orientalis*, *Heterosminthus orientalis*, *Protolactaga grabau*, *Gobicricetodon flynni* and *Stenofiber hesperus* are also present in the classical Tunggur fauna (Qiu, 1996).

DM02 (also DM11) level: The fauna is very similar to the DM01 fauna (Table 1). Large mammals are represented by the three cervoids *Micromeryx*, *Stephanocemas* and *Euprox*. Small mammals are abundant and diverse. There are four lagomorphs (*Desmatolagus* sp. indet., *Bellatona forsythmajori*, *Ochotona* sp. indet., and *Alloptox* sp. indet.), two insectivores (*Mioechinus* sp. indet., *Talpidae* gen. et sp. indet.), and more than ten rodents (*Protolactaga* sp. indet., *Lophocricetus* sp. indet., *Eozapus* sp. indet., *Gobicricetodon* sp. indet., *Prosiphneus qiui*, *Nannocricetus wuae*, *Cricetidae* gen. et sp. nov., *Gliridae* gen. et sp. indet., *Eomyidae* gen. et sp. indet., *Aplodontidae* gen. et sp. indet., *Castoridae* gen. et sp. indet.). The faunal composition is similar to that of the Tunggur fauna (Qiu, 1996). However *Lophocricetus*, *Prosiphneus* and *Ochotona* are more abundant and appear to have replaced *Heterosminthus*, *Plesiodipus* and *Bellatona*, respectively, as the dominant forms. *Heterosminthus* is confined to the early and middle Miocene, while *Lophocricetus* is known from the late Miocene and early Pliocene (Qiu et al., 2008). *Prosiphneus*, widely accepted as a successor to *Plesiodipus*, is documented mainly from late Miocene and later faunas. *Nannocricetus wuae* (Zhang et al., 2011b) is the most primitive species of the genus found till now. Compared with the faunas from the Bahe Formation, e.g. those from Loc.12 and Loc.19, this fauna appears earlier, with typical middle Miocene survivors such as *Protolactaga*, *Gobicricetodon*, *Micromeryx? Desmatolagus*, and *Alloptox*, as well

as a primitive species of *Nannocricetus*. The age of the DM02 fauna is most probably between those of the Tunggur fauna and faunas from the lower part of the Bahe formation. Considering the dominance of *Ochotona*, *Lophocricetus*, *Nannocricetus* and *Prosiphneus*, which have been recorded from typical late Miocene localities, we suggest the age of the DM 02 fauna to be earliest late Miocene.

5. Paleomagnetic analysis

5.1. Methods

Samples for paleomagnetic analysis were collected from the two sections at 83 sites in total. The stratigraphic intervals range from 0.1 m to 1.9 m with an average of 0.45 m in the eastern section and 0.7 m in the western section, depending on the availability of suitable exposures. In the field, the samples were collected as oriented hand samples and later sub-sampled in the laboratory into standard cube-shaped ($2 \times 2 \times 2 \text{ cm}^3$) or cylindrical specimens (2.2 cm high and 2.54 cm diameter). The dried hand samples were extremely fragile and therefore a non-magnetic silicone adhesive was used to fasten and waterproof the samples before they were fixed in gypsum when processing at the Paleomagnetic Laboratory "Fort Hoofddijk", Utrecht University (UU), Netherlands. Subsequently, the fixed samples were sub-sampled into the standard cylindrical specimens.

At the UU, a selected number of samples were measured to determine the rock magnetic properties whilst all samples from the sections were measured for magnetostratigraphy. For the rock magnetic properties, thermomagnetic runs were measured in air with a modified horizontal translation type Curie balance with a sensitivity of approximately $5 \times 10^{-9} \text{ Am}^2$ (Mullender et al., 1993). A few milligrams of bulk sample were put into a quartz glass sample holder and were held in place by quartz wool. The measurements were carried out up to a temperature of 700 °C with heating and cooling rates of 10 °C/min. The initial susceptibility of each sample was measured on the Kappabridge KLY-2 (UU) ($4 \times 10^{-8} \text{ SI}$) and on the SM100 Portable Magnetic Susceptibility Meter (University of Helsinki, UH) (used frequency: 1 kHz; used field intensity: 320 A/m; sensitivity: $2 \times 10^{-7} \text{ SI}$).

The natural remanent magnetization (NRM) was thermally demagnetized in UU, using incremental heating steps of 50 °C below and 30 °C above 240 °C, in a laboratory-built shielded furnace. NRM and the remaining magnetization after each demagnetization step of the samples was measured on a horizontal 2G Enterprises DC SQUID cryogenic magnetometer (noise level $3 \times 10^{-12} \text{ A/m}$; UU). Eight supplementary block samples from the topmost eastern section between 32.65 and 35.95 m were analyzed at the Solid Earth Geophysics research laboratory of University of Helsinki (UH). The block samples were cut into cubic specimens ($2 \times 2 \times 2 \text{ cm}^3$), which were demagnetized by 17

incremental alternating field steps using 2G Enterprises horizontal DC SQUID cryogenic magnetometer (noise level 10^{-7} A/m).

Demagnetization results are plotted on orthogonal vector diagrams (Zijderveld, 1967) and characteristic remanent magnetization (ChRM) directions are calculated using principal component analysis (Kirschvink, 1980) based on at least four successive demagnetization steps.

5.2. Rock magnetic properties

The magnetic minerals in the sediments were identified from the Curie balance measurements. A selection of samples from different types of lithologies were analyzed for this purpose (Fig. 5). Since most of the samples were taken in the more consolidated and less weathered parts of the finer grained floodplain deposits, the rock magnetic analysis show rather consistent results. The Curie balance measurements indicate that the initial total magnetization is low in most of the samples (Fig. 5). In addition, the contribution of the paramagnetic minerals is dominant. Blocking temperatures are in the range of 550–580 °C (Fig. 5c and d) suggesting that magnetite (Dunlop and Özdemir, 1997) is the dominant carrier in the magnetization of the sediments at the Damiao site. In some samples, higher blocking temperatures between 620

and 650 °C are found suggesting the presence of hematite (Fig. 5a and b).

5.3. Demagnetization results

Depending on the lithofacies, the NRM intensities vary between 240 and 22,000 $\mu\text{A/m}$, with highest values for the red siltstones. Most of the samples show a reliable paleomagnetic signal (Fig. 6). The Zijderveld diagrams of the thermally demagnetized samples reveal the presence of two to three magnetic components (Fig. 6a–c and f–h), whereas the AF demagnetized samples show two components (Fig. 6d and e). In thermal demagnetization a first randomly oriented component is removed around 100 °C. A second normal oriented component is removed between 170 and 270 °C most probably representing a viscous overprint inherited from the present-day field ($D = 355^\circ$ $I = 61^\circ$). The third component is interpreted to represent the characteristic remanent magnetization (ChRM) direction, which was calculated using at least four thermal demagnetization steps in the range from 270 °C to 690 °C (Fig. 6b and c, majority of the samples) or to 570 °C to 630 °C (Fig. 6a and f) suggesting hematite and magnetite, respectively. The samples showing hematite mostly consist of red silt- and mudstones, whereas the samples showing magnetite consist of very fine to coarse grained sandstone.

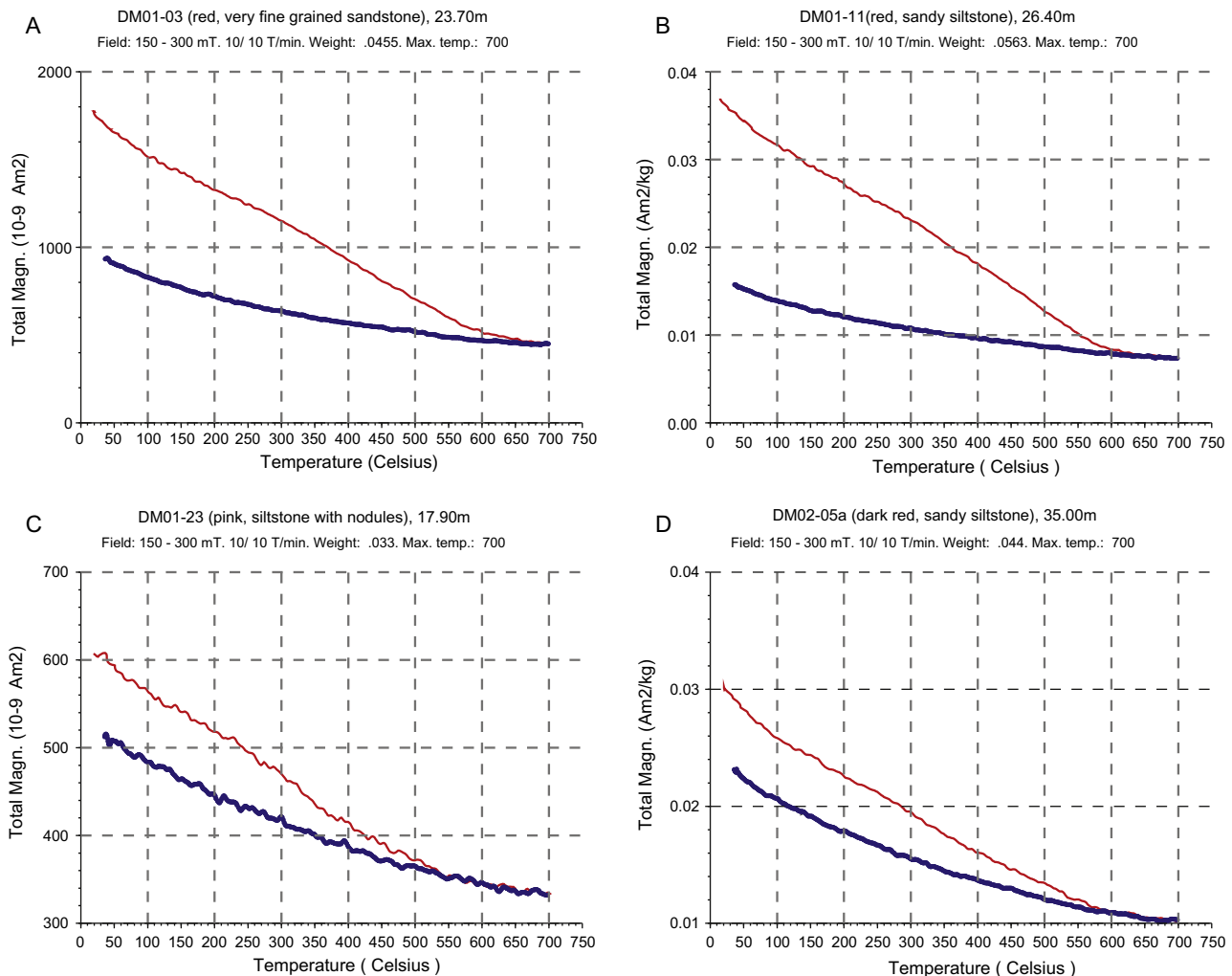


Fig. 5. (A–D) Representative thermomagnetic runs for samples from different lithologies at the Damiao study site. The red curve represents the heating and blue the cooling at a rate of 10 °C/min, respectively. A single run was set up to 700 °C at cycling fields of 150 and 300 mT. The sample name, its corresponding lithology and stratigraphic level (in m) are indicated. See text for details.

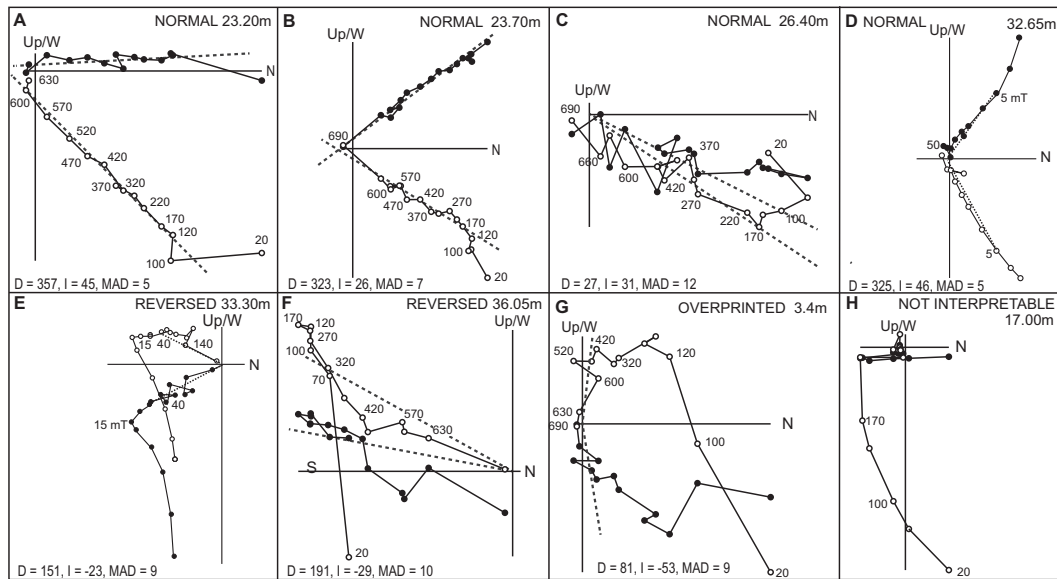


Fig. 6. Representative demagnetization diagrams for selected specimens. (A–F) examples of samples that show characteristic remanence component (ChRM). (G–H) example of samples that did not show ChRM. Per sample: The name and stratigraphic level of a sample is given in the top right corner. In the lower left corner the declination, inclination and Mean Angular Deviation (MAD) is shown. In the diagram itself the values along the vectors are given in °C (A–C, and F–H) or in mT (D and E). See text for details.

Progressive AF demagnetization removed an initial low coercivity component in 5–7.5 mT peak fields. Vector diagrams decayed to origin and a high coercivity ChRM component was isolated between 15 and 160 mT suggesting magnetite as remanence carrier (Fig. 6d and e).

Analyzed declination and inclination results of all sections are plotted in stratigraphic order in Figs. 3 and 4. Samples showing maximum angular deviation (MAD) values larger than 20° and samples with unconvincing ChRM directions were considered unreliable and are indicated with open circles. Samples that could not be interpreted or that had orientation problem (e.g., Fig. 6g and h) are indicated with crosses. Non-interpretable and intervals lacking data are represented by gray shaded areas in the polarity columns.

The western Damiao section consists of at least two magnetozones (Fig. 3). The base of the section has a reversed polarity whereas the top part is dominantly normal. Within the top part, two gray shaded intervals are present indicating that no polarity could be determined. However, the topmost part likely indicates the presence of a reversed polarity but this reversal is based on one sample only with a relatively poor data quality.

At least four magnetozones, two normal and two reversed polarities, have been determined in the eastern section (Fig. 4). The upper half of the section shows dominantly a reversed polarity with a short normal in between two reversed. The lower half shows a normal polarity. The gray shaded zones within the top most part of the section and within the lower long normal cannot be resolved.

6. Discussion and conclusions

6.1. Correlation of magnetozones to the ATNTS

6.1.1. The western section

By faunal comparison, the DM16 fauna should be earlier than the Shanwang biota, which is recently estimated to 17 Ma based on $^{39}\text{Ar}/^{40}\text{Ar}$ ages of the basalts above, below and within the Shanwang Formation (He et al., 2011). The comparable and maybe slightly younger fauna, the lower Aorban fauna, was paleomagnetically dated to C6n (19.722–18.748 Ma) (Liddicoat et al., 2007;

Wang et al., 2009) although parts of that section did not yield robust paleomagnetic results. Detailed paleomagnetic and biostratigraphic work has been carried out in the Tiersihabahe section, Junggar Basin, Xinjiang (Zhang et al., 2006; Sun et al., 2010; Ye et al., 2012) encompassing early Miocene localities S-II and S-III. The DM16 fauna is almost certainly later than S-II that is interpreted as earliest Miocene (Meng et al., 2006; Ye et al., 2012), and most comparable with those from S-III. This evidence supports a plausible correlation to the Astronomically Tuned Neogene Time Scale (ATNTS) (Fig. 7; Lourens et al., 2004; Gradstein et al., 2012), suggesting that reversed magnetozone in the base of the western section may correspond to Early Miocene chron C6Ar (21.083–20.709 Ma). Alternatively, it may be correlated to chron C6An.1r, having an age of 20.439–20.213 Ma.

6.1.2. The eastern section

Given the constraint that the mammalian assemblage found in DM01 is comparable with the latest middle Miocene Tunggur fauna and DM02 fauna is associated with earliest late Miocene and predating the lowermost Bahe Fm localities at ca. 10.7 Ma (Zhang et al., 2013), a unique correlation with the ATNTS is feasible. As a consequence, the normal polarity magnetozone associated with DM 01 (and DM 03) is correlated to the late middle Miocene chron C5An.1n (12.014–12.116 Ma) whereas the normal polarity associated with DM02 can be correlated to early late Miocene chron C5r.2n (11.554–11.614 Ma). An alternative correlation covering late middle Miocene would place the long normal to the chron C5AAn and the short normal polarity to CAr.2n. This correlation is considered to be unlikely, as it suggests much older ages for DM01 (ca 13.2 Ma) and DM02 (ca 12.8 Ma) and therefore conflicting with the early late Miocene age indicated by mammal remains in the DM02.

The resultant sediment accumulation rate for C5r.3r through C5r.2n is excessively low (<1 cm/kyr) but logical as these zones correspond to low energy floodplain environments that tend to have intermittent sedimentation and overall low sedimentation rates. The low sedimentation rate is also consistent with respect to those recorded elsewhere in the Erlian Basin: an accumulation rate of 1.2 cm/kyr has been determined for a Paleocene–Eocene

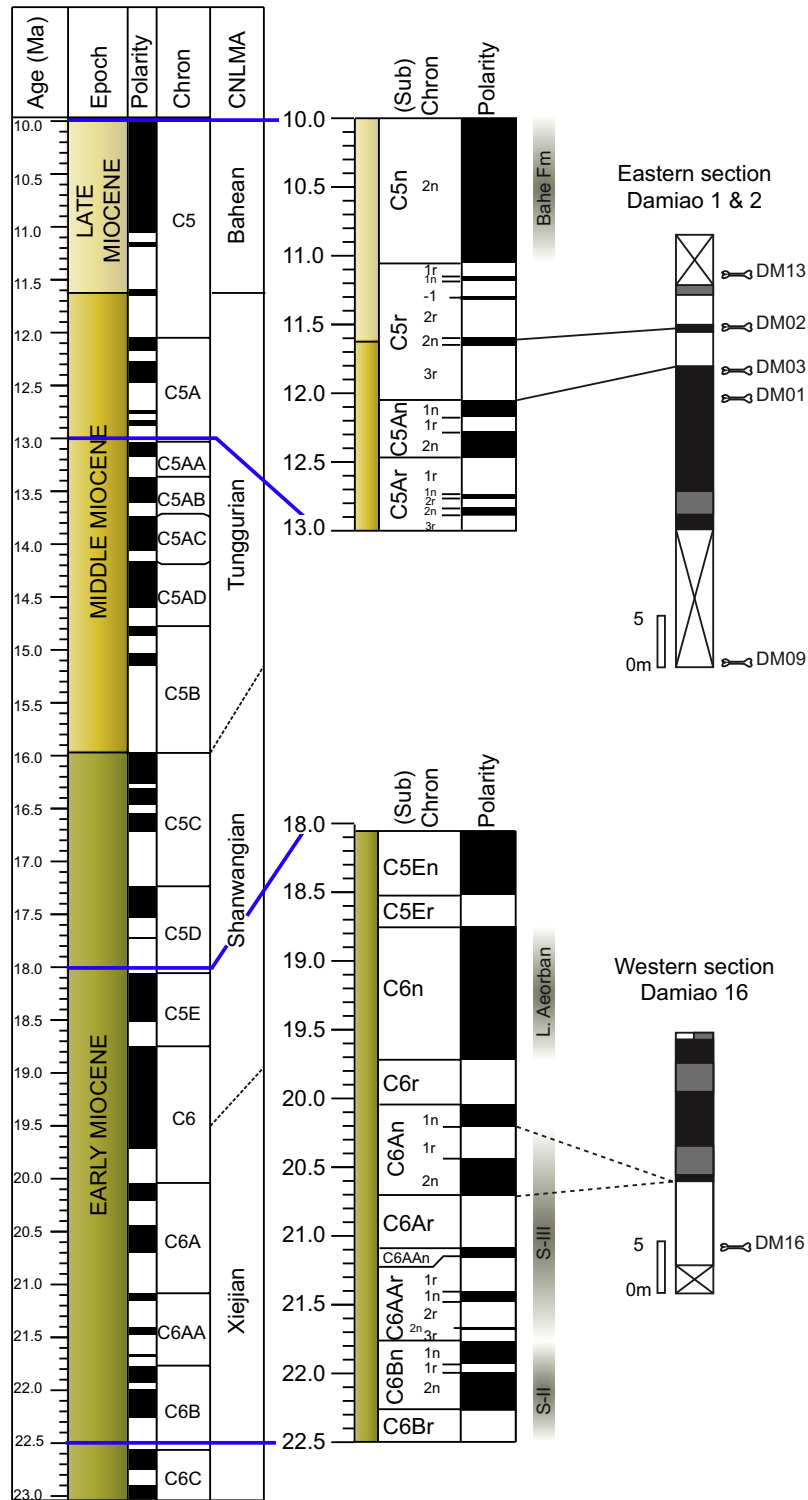


Fig. 7. Correlations of the Damiao magnetic polarity zones to the Astronomically Tuned Neogene Time Scale (ATNTS) (Lourens et al., 2004; Gradstein et al., 2012) and Chinese Neogene Land Mammal Ages (CNLMA) (Qiu Z.X. et al., 2013). The hatched boxes represent localities and/or deposits referred to in the text – Bahe Fm (Zhang et al., 2013), Lower Aeorban (Liddicoat et al., 2007; Wang et al., 2009), S-III and S-II (Meng et al., 2006; Ye et al., 2012). See Section 6.1 for discussion of the rationale for these correlations.

sequence in Bayan Ulan (Bowen et al., 2005); 6.3 cm/kyr and 4.7 cm/kyr for the Middle Miocene Tunggur Formation localities Moergen and Tairum Nor, respectively (Wang et al., 2003); and 6 cm/kyr for the lower Pliocene Gaotege beds (O'Connor et al., 2008). Nevertheless, the accumulation rate in Damiao is based on two magnetochrons only and large variation in rates through the sequence is expected.

6.2. Environmental trends and the presence of primates

The large mammal community structure shows a relatively stable pattern with dominance of cervoids excluding the possibility of widespread open environments for the Damiao sequence. The presence of humid-favouring primate *Pliopithecus* at DM01 indicates relatively closed conditions for the latest Middle Miocene

(Zhang and Harrison, 2008). Warm and humid environments for DM01 level are also suggested by the presence of an anchitheriine horse and the cervid *Euprox altus*, whose dental morphology indicates a more browsing diet relative to other contemporaneous *Euprox* (Wang and Zhang, 2011).

Based on sedimentological data, the Damiao sequence is characterized as a fluvial environment. The bulk of the fine-grained deposits in the sequence are red clay and siltstones with variable concentrations of nodular carbonate suggesting well-drained floodplains and groundwater evaporation. The thinly laminated fines at DM16 can be related to still water bodies but the ponded areas cannot necessarily be related to climate but may reflect floodplain morphology and drainage. A more humid climate associated with the pliopithecoid locality is suggested by the occurrence of abundant goethite and manganese staining in the fluvial conglomerates and interdigitating fine-grained beds at the locality DM01 environs. Manganese oxides are more typical in soils with impeded drainage such that soil conditions alternate between reducing and oxidizing (Kraus and Hasiotis, 2006). The reworked pedogenic nodules in the conglomerates however indicate that climate was seasonally dry (cf. Van Itterbeeck et al., 2007).

Pliopithecids have a wide geographical distribution from the Iberian Peninsula to China during the Miocene (Harrison, 2013). In China, the other middle Miocene sites yielding pliopithecids are in Tongxin, Ningxia Hui Autonomous Region (Harrison et al., 1991), Tiersihabahe in the northern Junggar Basin of Xinjiang Uygur Autonomous Region (Wu et al., 2003) and in Laogou, Gansu Province (Deng, 2003). Eronen and Rook (2004) studied the European primate fossil record and noted that the pliopithecids are found only in humid habitats, in accordance with their dentition and limb anatomy indicating an arboreal lifestyle (Agustí and Antón, 2002, p. 139). The occurrence of pliopithecoid primates after the middle Miocene climatic optimum in Central Asia poses an interesting paradox as it appears to contradict the contemporary trend of strengthening of climatic zones and increased aridification of the mid-latitudes in extensive areas since Early Miocene (e.g. Guo et al., 2002; Sun et al., 2010). It is, however, consistent with the local sedimentological evidence reported here and with the regional interpretation of large mammal proxy data by (Liu et al., 2009), suggesting that, while a distinctive dry belt developed in the mid latitudes, humid areas remained in the southern and northern parts of China. At the very least, the presence of pliopithecoid primates points to the occurrence of locally humid environments within the regionally arid context, and thus to more spatial heterogeneity than has often been assumed.

Acknowledgements

We thank Elina Hernesniemi, Aleksis Karme, Liu Yan, Luo Zhiqiang, Hannele Peltonen, Leena Sukselainen, and Yang Xingkai for providing assistance in the field and Pasi Heikkilä for helpful discussions. We thank Pierre-Olivier Antoine and an anonymous reviewer for thorough and constructive comments. The research was funded by Waldemar von Frenckell Foundation, the Academy of Finland, NSFC (41072004), and Science and Technology Ministry of China (2012CB821904).

References

Agustí, J., Antón, M., 2002. Mammoths, Sabertooths, and Hominids: 65 Million Years of Mammalian Evolution in Europe. Columbia University Press, p. 313.

Andersson, J.G., 1923. Essays on the Cenozoic of Northern China. Mem. Geol. Surv. China Ser. A 3, 1–152.

Andrews, R.C., 1932. The new conquest of Central Asia, a narrative of the explorations of the Central Asiatic Expeditions in Mongolia and China, Natural History of Central Asia. Am. Mus. Nat. History 1, 1–678.

Bi, S.D., 1999. Metaxallorix from the Early Miocene of North Junggar Basin, Xinjiang Uygur Autonomous Region, China. Vertebrata Palasiatica 37, 140–155.

Bowen, G.J., Koch, P.L., Meng, J., Ye, J., Ting, S., 2005. Age and correlation of fossiliferous late Paleocene – early Eocene strata of the Erlan Basin, Inner Mongolia, China. Am. Mus. Novit. 3464, 1–26.

Bureau of Geology and Mineral Resources of Nei Mongol autonomous region, 1991. Regional Geology of Nei Mongol (Inner Mongolia) Autonomous Region, People's Republic of China. Geological Memoirs Series, vol. 1, 25. Geological Publishing House, Beijing, p. 725.

Deng, T., 2003. New material of *Hispanotherium matritense* (Rhinocerotidae, Perissodactyla) from Laogou of Hezheng County (Gansu, China), with special reference to the Chinese Middle Miocene elasmotheres. Geobios 36, 141–150.

Dunlop, D.J., Özdemir, O., 1997. Rock Magnetism, Fundamental and Frontiers. Cambridge University Press, Cambridge, p. 592.

Eberth, D.A., Miall, A.D., 1991. Stratigraphy, sedimentology and evolution of vertebrate-bearing, braided to anastomosed fluvial systems, Cuttler Formation (Permian to Pennsylvanian), north-central New Mexico. Sed. Geol. 72, 225–252.

Eronen, J.T., Rook, L., 2004. The Mio-Pliocene European primate fossil record: dynamics and habitat tracking. J. Hum. Evol. 47, 323–341.

Gradstein, F.M., Ogg, J.G., Schmitz, M.D., Ogg, G.M., 2012. The Geologic Time Scale. Elsevier, Amsterdam.

Guo, Z.T., Ruddiman, W.F., Hao, Q.Z., Wu, H.B., Qiao, Y.S., Zhu, R.X., Peng, S.Z., Wei, J.J., Yuan, B.Y., Liu, T.S., 2002. Onset of Asian desertification by 22 Myr ago inferred from loess deposits in China. Nature 416, 159–163.

Harrison, T., 2013. Catarrhine origins. In: Begun, D.R. (Ed.), A Companion to Paleanthropology. Wiley Blackwell, Oxford, pp. 376–396.

Harrison, T., Delson, E., Guan, J., 1991. A new species of *pliopithecus* from the middle Miocene of China and its implications for early catarrhine zoogeography. J. Hum. Evol. 21, 329–361.

He, H.Y., Deng, C.L., Pan, Y.X., Deng, T., Luo, Z.H., Sun, J.M., Zhu, R.X., 2011. New ³⁹Ar/⁴⁰Ar dating results from the Shanwang Basin, eastern China: constraints on the Shanwang Formation and the associated biota. Phys. Earth Planet. Inter. 187, 66–75.

Kimura, Y., 2010. New material of Dipodid rodents (Dipodidae, Rodentia) from the early Miocene of Gashunynadege, Nei Mongol, China. J. Verteb. Paleontol. 30, 1860–1873.

Kirschvink, J.L., 1980. The least squares lines and plane analysis of palaeomagnetic data. Geophys. J. Roy. Astron. Soc. 62, 699–718.

Kraus, M.J., Gwinn, B., 1997. Facies and facies architecture of Paleogene floodplain deposits, Willwood Formation, Bighorn basin, Wyoming, USA. Sed. Geol. 114, 33–54.

Kraus, M.J., Hasiotis, S.T., 2006. Significance of different modes of rhizolith preservation to interpreting paleoenvironmental and paleohydrologic settings: examples from Paleogene paleosols, Bighorn Basin, Wyoming, USA. J. Sediment. Res. 76, 633–646.

Li, C., Qiu, Z., 1980. Early Miocene mammalian fossils of Xining Basin, Qinghai. Vertebrata Palasiatica 18, 198–214.

Liddicoat, J.C., Wang, X.M., Qiu, Z.D., Li, Q., 2007. Recent paleomagnetic and magnetostratigraphic investigations on and around the Tunggur tableland, central Nei Mongol (Inner Mongolia). Vertebrata Palasiatica 45, 110–117.

Lin, C., Eriksson, K., Li, S., Wan, Y., Ren, J., Zhang, Y., 2001. Sequence architecture, depositional systems, and controls on development of lacustrine basin fills in part of the Erlan Basin, Northeast China. AAPG Bull. 85, 2017–2043.

Liu, L., Eronen, J.T., Fortelius, M., 2009. Significant mid-latitude aridity in the middle Miocene of East Asia. Palaeogeogr. Palaeoclimatol. Palaeoecol. 279, 201–206.

Lourens, L., Hilgen, F., Shackleton, N.J., Laskar, J., Wilson, D., 2004. The Neogene Period. In: Gradstein, F.M., Ogg, J.G., Smith, A. (Eds.), A Geologic Time Scale 2004. Cambridge University Press, Cambridge, UK, pp. 409–440.

Luo, X.Q., Chen, Q.T., 1990. Preliminary study on geochronology for Cenozoic basalts from Inner Mongolia. Acta Petrologica et Mineralogica 9, 37–46 (in Chinese).

Meng, J., Wang, B.Y., Bai, Z.Q., 1996. A new middle Tertiary mammalian locality from Sunitezuoqi, Nei Mongol. Vertebrata Palasiatica 34, 297–304 (in Chinese with English abstract).

Meng, Q.R., Hu, J.M., Jin, J.Q., Zhang, Y., Xu, D.F., 2003. Tectonics of the late Mesozoic wide extensional basin system in the China – Mongolia border region. Basin Res. 15, 397–415.

Meng, J., Ye, J., Wu, W.Y., Yue, L.P., Ni, X.J., 2006. A recommended boundary stratotype section for Xiejian Stage from northern Junggar Basin: implications to related bio-chronostratigraphy and environmental changes. Vertebrata Palasiatica 44, 205–236 (in Chinese with English summary).

Miall, A.D., 1996. The Geology of Fluvial Deposits: Sedimentary Facies, Basin Analysis and Petroleum Geology. Springer-Verlag, Berlin, p. 582.

Mullender, T.A.T., van Velzen, A.J., Dekkers, M.J., 1993. Continuous drift correction and separate identification of ferromagnetic and paramagnetic contributions in thermomagnetic runs. Geophys. J. Int. 114, 663–672.

O'Connor, J.K., Prothero, D.R., Wang, X.M., Li, Q., Qiu, Z.D., 2008. Magnetic stratigraphy of the lower Pliocene Gaoztege beds, Inner Mongolia. New Mexico Mus. Nat. History Sci. Bull. 44, 431–436.

Qiu, Z.D., 1996. Middle Miocene Micromammalian Fauna from Tunggur, Nei Mongol. Science Press, Beijing, pp. 1–216.

Qiu, Z.X., Gu, Z., 1988. A new locality yielding mid-Tertiary mammals near Lanzhou, Gansu. Vertebrata Palasiatica 26, 198–213.

Qiu, Z., Storch, G., 2000. The early Pliocene micromammalian fauna of Bilike, Inner Mongolia, China (Mammalia: Lipotyphla, Chiroptera, Rodentia, Lagomorpha). Senckenb. Lethaea 80, 173–229.

Qiu, Z.D., Wang, X.M., Li, Q., 2006. Faunal succession and biochronology of the Miocene through Pliocene in Nei Mongol (Inner Mongolia). Vertebrata Palasiatica 44, 164–181.

- Qiu, Z.D., Zheng, S.H., Zhang, Z.Q., 2008. Sciurids and zaptodids from the Late Miocene Bahe Formation, Lantian, Shaanxi. *Vertebrata Palasiatica* 46, 111–123.
- Qiu, Z.D., Wang, X., Li, Q., 2013. Neogene faunal secession and biochronology of Central Nei Mongol (Inner Mongolia). In: Wang, X.M. et al. (Eds.), *Fossil Mammals of Asia: Neogene biostratigraphy and chronology*. Columbia University Press, New York, pp. 155–186.
- Qiu, Z.X., Qiu, Z.D., Deng, T., Li, C.K., Zhang, Z.Q., Wang, B.Y., Wang, X., 2013. Neogene land mammal stages/ages of China: Toward the goal to establish an Asian Land Mammal Stage/Age scheme. In: Wang, X.M. et al. (Eds.), *Fossil Mammals of Asia: Neogene Biostratigraphy and Chronology*. Columbia University Press, New York, pp. 29–90.
- Sun, J.M., Ye, J., Wu, W.Y., Ni, X.J., Bi, S.D., Zhang, Z.Q., Liu, W.M., Meng, J., 2010. Late Oligocene – Miocene mid-latitude aridification and wind patterns in the Asian interior. *Geology* 38, 515–518.
- Teilhard de Chardin, P., 1926a. Étude géologique sur la région du Dalai-Nor. *Mémoires de la Société Géologique de France* 7, 1–56.
- Teilhard de Chardin, P., 1926b. Description de mammifères tertiaires de Chine et de Mongolie. *Annales de Paléontologie* 15, 1–52.
- Tong, Y., 1989. A new species of *Sinolagomys* (Lagomorpha, Ochotonidae) from Xinjiang. *Vertebrata Palasiatica* 27, 103–116.
- Van Itterbeeck, J., Missiaen, P., Folie, A., Markevich, V.S., Van Damme, D., Guo, D.Y., Smith, T., 2007. Woodland in a fluvio-lacustrine environment on the dry Mongolian Plateau during the Paleocene: evidence from the mammal bearing Subeng section (Inner Mongolia, PR China). *Palaeogeogr. Palaeoclimatol. Palaeoecol.* 243, 55–58.
- Wang, L.H., Zhang, Z.Q., 2011. A new species of *Euprox* (Cervidae, Mammalia) from the Middle Miocene of Damiao, Nei Mongol, China. *Vertebrata Palasiatica* 49, 365–376.
- Wang, X.M., Qiu, Z.D., Opdyke, N.D., 2003. Litho-, bio-, and magnetostratigraphy and paleoenvironment of Tunggur Formation (Middle Miocene) in Central Inner Mongolia, China. *Am. Mus. Novit.* 3411, 1–31.
- Wang, X.M., Qiu, Z.D., Li, Q., Tomida, Y., Kimura, Y., Tseng, Z.J., Wang, H.J., 2009. A new early to late Miocene fossiliferous region in central Nei Mongol: lithostratigraphy and biostratigraphy in Aorban strata. *Vertebrata Palasiatica* 47, 111–134.
- Wu, W.Y., Meng, J., Ye, J., 2003. The discovery of *Pliopithecus* from northern Junggar Basin, Xinjiang. *Vertebrata Palasiatica* 41, 76–86.
- Xu, X.W., Ma, Z.Y., 1992. Geodynamics of the Shanxi Rift system, China. *Tectonophysics* 208, 325–340.
- Ye, J., Wu, W.Y., Ni, X.J., Bi, S.D., Meng, J., 2012. The Duolebulejin section of Northern Junggar Basin and its stratigraphic and environmental implication. *Scientia Sinica Terrae* 42, 1523–1532 (In Chinese).
- Zhang, Z.Q., Harrison, T., 2008. A new middle Miocene pliopithecoid from Inner Mongolia, China. *J. Hum. Evol.* 54, 444–447.
- Zhang, R., Yue, L.P., Wang, J.Q., 2006. Magnetostratigraphic dating of Cenozoic mammalian fossils in Junggar Basin, northwest China. *Chin. Sci. Bull.* 51, 842–847 (in Chinese).
- Zhang, Z.Q., Wang, L.H., Kaakinen, A., Liu, L.P., Fortelius, M., 2011a. Miocene mammalian faunal succession from Damiao, central Nei Mongol and the environmental changes. *Quat. Sci.* 31, 608–613.
- Zhang, Z.Q., Wang, L.H., Liu, Y., Liu, L.P., 2011b. A new species of Late Miocene hamster (Cricetidae, Rodentia) from Damiao, Nei Mongol. *Vertebrata Palasiatica* 49, 201–209.
- Zhang, Z.Q., Kaakinen, A., Liu, L.P., Lunkka, J.P., Sen, S., Gose, W.A., Qiu, Z.D., Zheng, S.H., Fortelius, M., 2013. Mammalian biochronology of the Late Miocene Bahe Formation. In: Wang, X.M. et al. (Eds.), *Fossil Mammals of Asia: Neogene Biostratigraphy and Chronology*. Columbia University Press, New York, pp. 187–202.
- Zijderveld, J.D.A., 1967. A.C. demagnetization of rocks: analysis of results. In: Collinson, D.W., Creer, K.M., Runcorn, S.K. (Eds.), *Methods in Paleomagnetism*. Elsevier, Amsterdam, pp. 254–286.